Poster #4593

# Inferring FGFR Status from H&E Images Using Digital Pathology to Identify Patients for Early-Stage Bladder Cancer Targeted Therapies


Albert Juan Ramon[1], Fatemeh Koochaki[1], Chaitanya Parmar[1], Patricia Raciti[2], Neil Beeharry[2], Christopher J. Medberry[3], Cheng Zhang[3], David Weingeist[4], Nicole Stone[5], Spyros Triantos[5], Joel Greshock[6], Kristopher A Standish[1]

Johnson and Johnson, [1]Data Sciences, Computer vision; [2]Oncology Translational Research; [3]Regulatory; [4]Oncology Diagnostics, [5]Oncology; [6]Data Sciences, Oncology; Raritan NJ 08869, USA;

Author contact information for questions and comments:

Albert Juan Ramon, PhD, Johnson and Johnson Innovative Medicine

ajuanram@its.jnj.com


## Key Takeaway

The MIA:BLC-FGFR algorithm enables rapid and accurate detection of FGFR status from routine H&E images, providing an encouraging alternative to conventional nucleic acid testing for NMIBC patients.

## Conclusions

**High Concordance:** MIA:BLC-FGFR shows strong agreement with nucleic acid testing methods and high generalizability across NMIBC risk categories / disease settings.

**Effective:** This AI-based solution offers quick and affordable FGFR testing, giving the ability to test any digitized slide from a tumor

Scan the QR code

Poster

https://www.congreshub.com/Oncology/AM2025/ErdaRIS/Ramon




**Acknowledgments**

The authors wish to express their gratitude to the Johnson & Johnson R&D Computer Vision, Oncology Diagnostics, Oncology Translational Research, Oncology Data Sciences, and Data Sciences Platforms teams for their contributions and support throughout this project. Their expertise and dedication greatly contributed to the project's results. We appreciate their involvement and positive impact.


res

## Introduction

- Clinical trials are ongoing to evaluate the efficacy of **FGFR** (Fibroblast Growth Factor Receptor) inhibitors in non-muscle-invasive bladder cancer (**NMIBC**), where genetic testing is not routine. Current nucleic acid-based tests used to detect **FGFR+** patients have limitations, including a slow turnaround time and high nucleic acid input requirement, especially in NMIBC, where tissue is often scarce. [1]
- This study aims to demonstrate the performance of an AI-based digital pathology algorithm, **MIA:BLC-FGFR**, adapted to detect **FGFR** alterations in **NMIBC** patients from routine hematoxylin and eosin (H&E) stained whole slide images (WSIs). This approach can provide a rapid, low-cost, and effective alternative to nucleic acid testing.

## Methods

- **MIA:BLC-FGFR** consists of an image quality control (**QC**) preprocessing stage, a Foundation Model (**FM**) pre-trained on ~55k unlabeled digital WSIs from various sources (multiple scanners, hospital systems, labs, diseases, tissue sites), and a Classification Module to enable inference of FGFR status from H&E-stained images. **Figure 1** below showcases the schematic of **MIA:BLC-FGFR**.
- The **QC** module first processes whole slide images by dividing them into non-overlapping 224x224 pixel tiles and discarding those with artifacts or insufficient tissue. This ensures only quality-controlled tiles are utilized.
- These high-quality tiles are then fed into the Foundation Model, which is based on a Vision Transformer architecture and trained using self-supervised learning to enhance accuracy for FGFR status [2].
- The Classification Module was trained on datasets (n=3,067) that included a mix of samples from multiple sources and disease stages (i.e., **NMIBC**, muscle-invasive and metastatic bladder cancer) and genetic classification provided by the QIAGEN therascreen® FGFR RGQ RT-PCR Kit. The algorithm was tuned to achieve a balanced specificity and sensitivity by selecting the operating point with highest F1 score (i.e., balanced sensitivity/specificity) in the training data.
- As part of this study, we then applied this model to WSIs of biopsies from 3 independent test datasets (n=578) with varied NMIBC disease settings (i.e., high risk (HR) or intermediate risk (IR)) to evaluate the performance at detecting **FGFR** status, quantified by the Area Under ROC Curve (AUC).

**Figure 1: MIA:BLC-FGFR Device Schematic [1]**

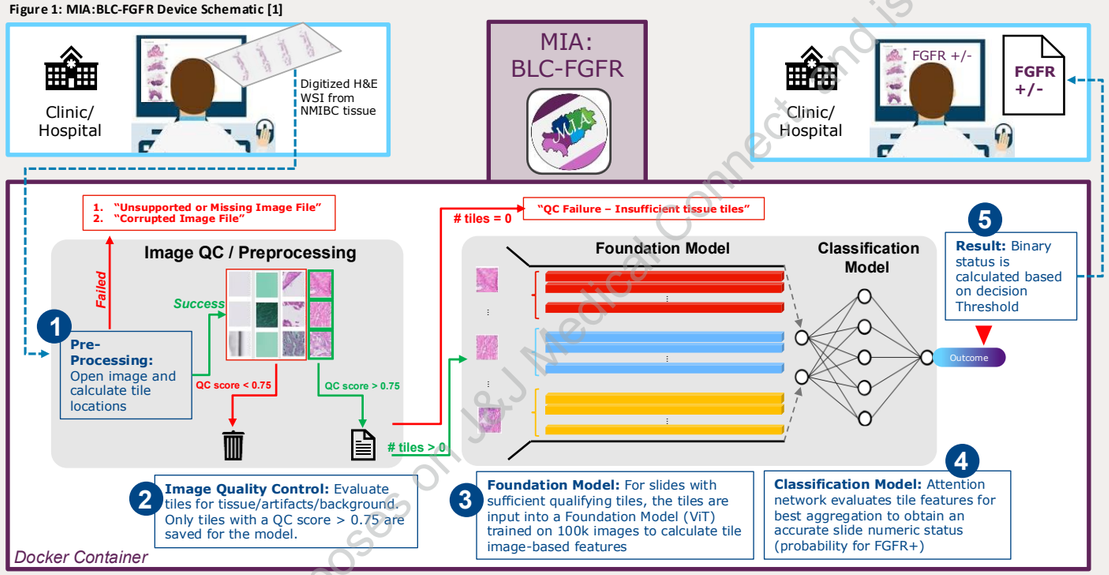


**Development and testing dataset statistics**

- The table below shows details of the datasets used for model development (i.e., training and tuning) and testing. Note that the datasets and methodology to pretrain the Foundation Model are different and fully independent those used to train the Classification Model.

**Table 1: Dataset characteristics**

| | Development Datasets (n=3,067) | Testing Datasets (n=578) |
|---|---|---|
| Purpose | TCGA, BLC3001, BLC2002, BLC2003 | BLC2003 (hold-out), Commercial Dataset, BLC1003 |
| Disease setting (FGFR+ %) | TCGA(MIBC), BLC3001(mUC), BLC2002(mUC): 2820 (10%); BLC2003(NMIBC): 247 (30%) | NMIBC: 578 (38%) |
| CRO Scanning Site | Switzerland (Geneva), US (Indianapolis), China (Shanghai), Japan (Tokyo), Singapore and TCGA sites | US (Indianapolis, Chicago, Nashville), EU (Belgium, Germany, Switzerland), China (Shanghai), Japan (Tokyo), Singapore |
| Reference test (% of WSIs by testing method) | NGS (~11%) +, V1 QIAGEN therascreen® FGFR RGQ RT-PCR Kit (~89%) | V1 QIAGEN therascreen® FGFR RGQ RT-PCR Kit (100%) |
| WSI Scanner | Leica Aperio AT2 or GT450 | Leica Aperio AT2 or GT450, 3DHistech P1000 |

## Results

**Concordance with tissue assay on 3 independent NMIBC datasets:**

- Table 2 below shows performance values for MIA:BLC-FGFR on three independent datasets, demonstrating high concordance with nucleic acid testing methods.

**Table 2: Concordance results**

| Test datasets: | BLC2003 (hold-out) | Commercial Dataset | BLC1003 |
|---|---|---|---|
| Disease setting | HR NMIBC | pT1 IR & HR NMIBC | IR NMIBC |
| Dataset size (FGFR+ %) | 245 (29.7%) | 163 (41%) | 169 (49%) |
| PPV | 53% | 64% | 80% |
| NPA | 66% | 71% | 82% |
| PPA | 89% | 73% | 76% |
| auROC | **85%** | **80%** | **86%** |

**Figure 2: Attention heatmap on a WSI from NMIBC tissue**

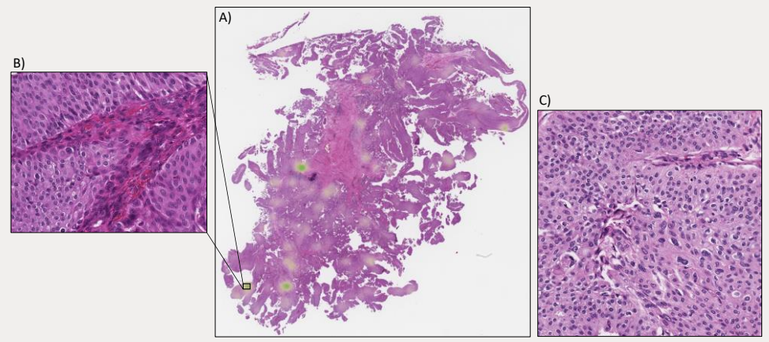


**Highly Scored Tiles (green) from WSI with FGFR Mutant Tumor, correctly classified by MIA**

- A) WSI shows exophytic papillary architecture with FGFR heatmap overlay.
- B) High scoring tile presents multilayered neoplastic urothelium with a fibrovascular core; cells have round to oval nuclei and eosinophilic cytoplasm with some clearing. [3]
- C) High scoring tile exhibits variable cell sizes, raisinoid nuclei, and perinuclear clearing, features linked to FGFR3 mutant high-grade urothelial carcinomas [3]


**References**

[1] Juan Ramon, A. et al. Development and deployment of a histopathology-based deep learning algorithm for patient prescreening in a clinical trial. Nature Communications, 15(1), 4690. (2024)

[2] Parmar, C. et al. Generalizable FGFR prediction across tumor types using self-supervised learning. J. Clin. Oncol. 41, e15057–e15057 (2023).

[3] Al-Ahmadie, H. A. et al. Somatic mutation of fibroblast growth factor receptor-3 (FGFR3) defines a distinct morphological subtype of high-grade urothelial carcinoma. J. Pathol. 224, 270–279 (2011).


Urothelial Cancer